Orthogonally Polarized Terahertz Wave Imaging with Real-Time Capability for Food Inspection

X. Yu[1], M. Endo[2], T. Ishibashi[3], M. Shimizu[4], S. Kusanagi[5], T. Nozokido[6], and J. Bae[1]
[1] Department of Engineering Physics, Electronics and Mechanics, Nagoya Institute of Technology
Gokiso-cho, Showa-ku, Nagoya 466-8555, Japan
[2] Aichi Center for Industry and Science Technology
1267-1 Akiai, Yakusa-cho, Toyota 470-0356, Japan
[3] NTT Electronics Techno Corporation
Atsugi R&D Center, 3-1 Morinosato-Wakamiya, Atsugi 243-0122, Japn
[4] NTT Electronics Corporation
6700-2 To, Naka 311-0122, Japan
[5] NTT Electronics Corporation
New Stage Yokohama, 1-1-32, Shin-urashima-cho, Kanagawa-ku, Yokohama 221-0031, Japan
[6] Graduate School of Science and Engineering for Research, University of Toyama
3190 Gofuku, Toyama 930-8555, Japan

***Abstract*- A terahertz imaging system operating at 0.3 THz has been developed for the purpose of detecting foreign substances in foods conveyed at a velocity of higher than 20 m/min. The imaging system has two Schottky barrier diode arrays which detect horizontally and vertically polarized terahertz waves independently and simultaneously. Experiments have shown that the imaging system can successfully obtain THz images with a diffraction limited resolution of 1 mm. It has also been shown that addition or subtraction of two images taken with perpendicularly polarized waves is effective to enhance the contrast of terahertz images.**

I. INTRODUCTION

Recently, inspection of foods using terahertz (THz) waves has attracted much attention because THz waves have a potential to overcome difficulties in conventional inspection methods such as using X-ray imagers and metal detectors [1]. These methods are almost useless to detect nonmetallic and low density foreign bodies such as plastics and insects [2]. Several authors have experimentally demonstrated that THz waves can detect these foreign bodies in foods [3], [4].

Food inspection in industrial production lines should be carried out at high speed and low cost. In order to fulfill these requirements, we have developed a high speed THz imaging system using continuous waves at 0.3 THz. In this THz imaging system, image data of foods are acquired using horizontally and vertically polarized THz waves independently and simultaneously. In general, since the shapes of foreign bodies are different from those of foods, they have different anisotropies [5]. Therefore, foreign bodies can be distinguished from foods by comparing the two polarization images even when they have similar dielectric constants. In this paper, our real-time imaging system utilizing orthogonally polarized THz waves is presented.

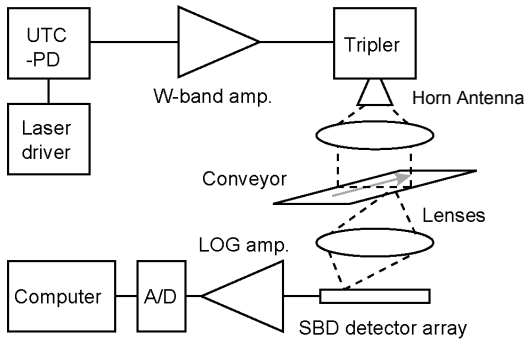

Figure 1. Schematics diagram of the 0.3 THz active imaging system for food inspection.

II. IMAGING SYSTEM

A. System configuration

Fig. 1 shows a schematic diagram of the THz imaging system. It consists of a continuous-wave THz source, lenses, a one-dimensional detector array, and a computer for image processing. This imaging system has been constructed assuming that objects, in our case, foods, are traveling by a conveyor belt and are inspected whether foreign substances are contained in the foods or not. The details of the system components are described in the following.

B. THz source and lenses

The THz source is composed of a uni-traveling-carrier photodiode (UTC-PD) mixer [6], a W-band amplifier, and a frequency tripler. The output frequency of the THz source is adjustable from 0.285 THz to 0.315 THz. The output power is 1.3 mW at 0.3 THz. Linearly polarized THz waves from the tripler are converted to circularly polarized waves and are emitted from a conical horn antenna.

In the imaging system, two sets of aspheric high-density polyethylene lenses were fabricated and used for illumination and image formation. The illumination lens converts a

circularly shaped beam emitted from the horn antenna into a line-shaped beam with a width of 1.1 mm and a length of 90 mm in the object plane on the conveyor. The objective consists of three lenses. The measured numerical aperture (NA) and magnification were 0.46 and 0.93, respectively.

In the experiments, a stepper-motor-driven linear actuator with an accuracy of better than 20 μm was used as a conveyor to precisely evaluate the performance of the THz imaging system.

C. *Schottky barrier diode detector array*

Fig. 2 is a photograph of the Schottky barrier diode (SBD) detector array we designed and fabricated. The SBD array is composed of 50 detector chips. The array pitch is 2 mm and the total length is 100 mm. The array fully covers a 90-mm-long illuminated section of the object plane. The *x*-*y* coordinate system we defined for this work is shown in Fig 2(a). The detector chips line up along the *x*-axis and the object to be imaged travels along the *y*-axis, resulting in two-dimensional image formation

Fig. 2(b) shows a photograph of the detector chip with dimensions of 1 mm x 2 mm. The chip integrated monolithically two slot antennas and two SBD's on a InP substrate with a thickness of 75 μm [7]. The spacing between the slots is 0.74 mm, which was so designed as to be a crosstalk level of less than -40 dB. These slot antennas can detect THz waves polarized in the *x*- and *y*- directions independently.

Fig. 3 shows the measured *H*-plane directivities of two slot antennas (Det. 1 and 2) chosen among the fabricated 100 antennas. The solid curve in Fig. 3 is the theoretical directivity calculated using a commercial simulator, ANSYS's HFSS. It is seen from the results that the slot antennas have a broader directivity of ±30 degrees as designed. This broader directivity is required to match the THz beam focused by the high NA objective to the antennas.

Measured sensitivities of the 100 detectors fluctuated from 400 V/W to 7000 V/W at 0.3 THz. This difference in sensitivities was compensated in image processing.

D. *Dynamic range and speed of data acquisition*

Signals detected by the SBD's were amplified in logarithmic (LOG) amplifiers and were sent to the computer though A/D converters for image processing. The measured dynamic range of the THz imaging system was 30 dB for the THz power of 1.3 mW at 0.3 THz.

In the THz imaging system, the outputs from the 50 LOG amplifiers generate a 90-mm-long line image with 50 pixels for each polarization state of THz waves. The minimum acquisition time for the two polarization line images was 84 μsec. If the data acquisition is done every 0.1 mm for objects traveling on a conveyor, the conveyor speed is equivalent to 72 m/min. This speed is high enough for use in the food industry. At present, unfortunately, commercial software, National Instruments' LabVIEW used for image processing limited the conveyor speed to less than 0.1 m/min. This problem can be solved using a high speed graphics processing unit.

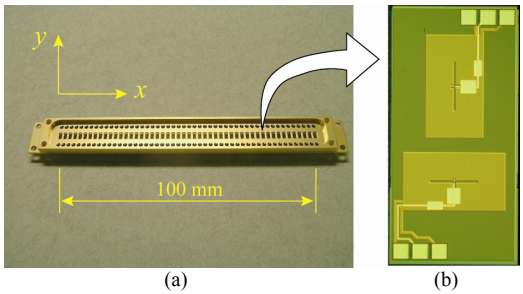

(a) (b)

Figure 2. (a) Photograph of the one dimensional SBD detector array and (b) magnified photo of the InP detector chip with a size of 1mm x 2mm.

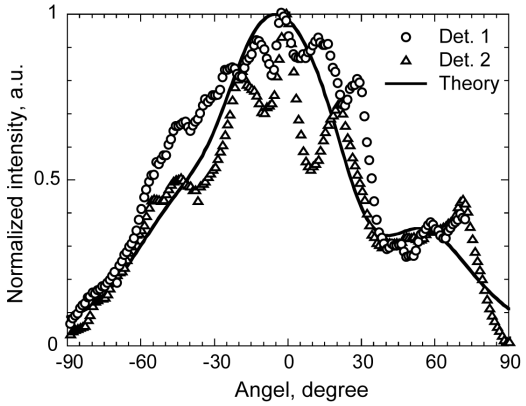

Figure 3. Measured *H*-plane directivity of the slot antennas. The solid curve is the theoretical directivity of the designed slot antenna.

III. IMAGING RESULTS

In order to evaluate the spatial resolution of the THz imaging system, a 1951 USFA resolution target provided by Edomund Optics Inc. was used as an object. This resolution target has several metal line patterns with different spacings on a quartz plate with dimensions of 76.2 mm x 76.2 mm x 1mm.

Fig. 4 compares (a) a photograph of the resolution target, (b) the THz image for the *x*-polarization, (c) the difference image between the two images for the *x*- and *y*- polarizations, and (d) the image added up the two images. The THz images in Fig. 4(b)-4(d) have data elements of 50 pixels with a spacing of 2.2 mm in the *x*-axis and 1000 pixels with a spacing of 0.1 mm in the *y*-axis.

In Fig. 4(b), the image resolution along the *y*-axis is much better than that along the *x*-axis. The resolution along the *x*-axis is 2.2 mm, which is determined by the detector pitch and the magnification of the objective. On the other hand, the resolution along the *y*-axis is determined by the NA of the objective and the wavelength of THz waves. From the measured NA of 0.46, the resolution of 1.3 mm in the *y*-axis is expected. The measured resolution was 1 mm, which was concluded from the fact that the metal lines with a width and a separation of 1 mm located at "a" in Fig. 4(a) are clearly resolved in the THz images in Fig. 4(b)-4(d). This result shows that the fabricated aspheric lenses have almost diffraction-limited resolution.

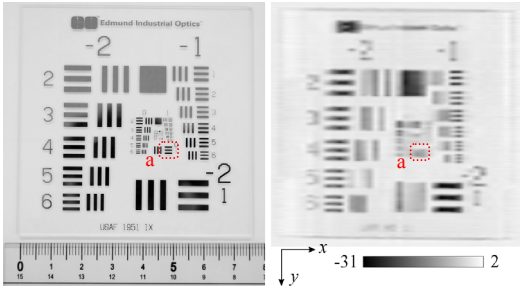

(a) Optical image (b) THz image for the *x*-polarization

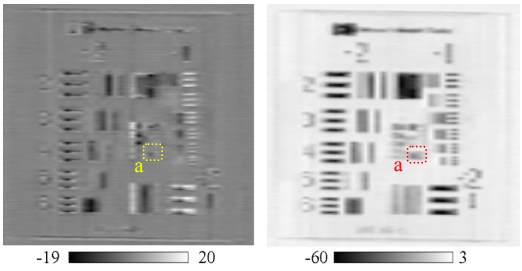

(c) THz difference image (d) THz added image

Figure 4. Measured images of a 1951 USFA resolution target, (a) optical image (photo), (b) the measured THz image for the *x*-polarization, (c) the deference image calculated by the subtraction of the *y*-polarization image from the *x*-polarization image, and (d) the image added up the *x*- and *y*-polarization images.

The difference image in Fig. 4(c) clearly shows the anisotropy of the metal lines. The white colored areas indicate that the signal amplitude for the *x*-polarization is larger than that for the *y*-polarization, and the black ones are the opposite. The anisotropy helps us easily recognize the metal edges. As pointed out in [5], anisotropy of objects with different shapes appears even when the objects themselves are made of uniform material. In general, foreign bodies have different shapes than foods so that the difference image for two orthogonal polarizations of THz waves could be effective to distinguish them from foods.

On the contrary, for inspection of foods with complex shapes, difference images may not be appropriate. In this case, polarization independent THz images are suitable. The image shown in Fig. 4(d) was generated by adding the image for the *x*-polarization to that for the *y*-polarization, so that the added image is independent of polarization of THz waves. In addition, as seen from Fig. 4(d), the contrast of THz image can be enhanced without any additional image processing.

Fig. 5 shows (a) a photograph of a chocolate bar with a caterpillar, and (b) the THz image of the chocolate bar put in a paper case shown in Fig. 5(a). Since the chocolate bar has a relatively complex shape, we adopted the added THz image for the measurement. In Fig. 5, the caterpillar is clearly distinguished from the chocolate in the paper case. This result indicates that the THz imaging system we have developed is useful for food inspection.

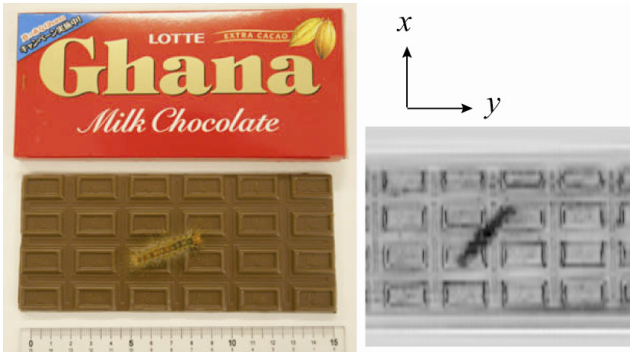

(a) Optical image (b) THz image

Figure 5. (a) Optical and (b) THz image of a caterpillar on a chocolate bar in a paper case. The THz image was created by adding up the measured *x*- and *y*-polarization images. The pixel size of the THz image is 50 x 1000.

IV. Conclusion

The orthogonally polarized THz-wave imaging system has been developed for food inspection at the frequency of 0.3 THz. The imaging system has a high spatial resolution of less than 2.2 mm and a real time capability. Its data acquisition time for a 90-mm long one line image with 50 pixels has been only 84 μsec. The THz imaging system can generate four different kinds of images, i.e. horizontal and vertical polarization images, and their subtraction and addition images. They can be used for sensitive detection of foreign bodies in foods. The usefulness of these THz images has been experimentally demonstrated.

Acknowledgment

This work has been conducted as one of "The Knowledge Hub" of AICHI, The Priority Research Projects.

References

[1] A. A. Gowen, C. O'Sullivan, and C. P. O'Donnell, "Terahertz time domain spectroscopy and imaging: Emerging techniques for food process monitoring and quality control," *Trends in Food Science &Technology*, vol. 25, no. 1, pp. 40-46, 2012.

[2] Z. Yan, Y. Ying, H. Zhang, and H. Yu, "Research progress of terahertz wave technology in food inspection," Terahertz Physics, Devices, and Systems, ed. M. Anwar, A. J. Demaria, and M. S. Shur, *Proc. of SPIE*, vol. 6373, 63730R, 2006.

[3] C. Jordens and M. Koch, "Detection of foreign bodies in chocolate with pulsed terahertz spectroscopy," *Optical Engineering*, vol. 47, no. 3, pp. 037003-1-5, 2008.

[4] W. H. Lee and W. Lee, "Food inspection system using terahertz imaging," *Microwave and Optical Tech. Lett.*, vol. 56, no. 6, pp. 1211-1214, 2014.

[5] N. C. J. van der Valk, W. A. M. van der Marel, and P. C. M. Planken, "Terahertz polarization imaging," *Optics Lett.*, vol. 30, no. 20, pp. 2820-2804, 2005.

[6] H. Ito, K. Yoshino, Y. Muramoto, H. Yamamoto, and T. Ishibashi, "Sub-Terahertz Transceiver Module Integrating Uni-Traveling-Carrier Photodiode, Schottky Barrier Diode, and Planer Circulator Circuit," *J. Lightwave Tech.*, vol. 28, no. 24, pp. 3599-3605, 2010.

[7] H. Ito, F. Nakajima, T. Ohno, T. furuta, T. Nagatsuma, and T. Ishibashi, "InP-Based Planar-Antenna-Integrated Schottky-Barrier Diode for Millimeter- and Sub-Millimeter-Wave Detection," *Japan. J. Appl. Phys.*, vol. 47, no. 8, pp. 6256-6261, 2008.